

A locally signed-distance preserving level set method (SDPLS) for moving interfaces

Mathis Fricke^{*1}, Tomislav Marić^{†1}, Aleksandar Vučković^{‡1}, and Dieter Bothe^{§1}

¹Mathematical Modeling and Analysis Group, TU Darmstadt

Abstract

It is well-known that the standard level set advection equation does not preserve the signed distance property, which is a desirable property for the level set function representing a moving interface. Therefore, reinitialization or redistancing methods are frequently applied to restore the signed distance property while keeping the zero-contour fixed. As an alternative approach to these methods, we introduce a novel level set advection equation that intrinsically preserves the norm of the gradient at the interface, i.e. the local signed distance property. Mathematically, this is achieved by introducing a source term that is proportional to the local rate of interfacial area generation. The introduction of the source term turns the problem into a non-linear one. However, we show that by discretizing the source term explicitly in time, it is sufficient to solve a linear equation in each time step. Notably, without adjustment, the method works naturally in the case of a moving contact line. This is a major advantage since redistancing is known to be an issue when contact lines are involved (see, e.g., Della Rocca and Blanquart, 2014). We provide a first implementation of the method in a simple first-order upwind scheme.

1 Introduction

Since the beginning of computational fluid dynamics in the 1960s, the field of computational multiphase flows has developed a variety of powerful specialized methods that allow the treatment of rather complex multiphase flow problems numerically. For example, modern multiphase flow methods allow to simulate flows with strong deformations and topological changes such as breakup and coalescence of droplets and the atomization of liquid jets. Moreover, additional transport processes are studied such as evaporation and condensation or the transport of surface-active substances leading to local Marangoni forces. Even reactive mass transfer processes involving dissolved chemical species are accessible with numerical simulation. Clearly, there is no single method that is equally suitable for all possible flow configurations. Instead, there is a variety of numerical methods with specific advantages and disadvantages for a given multiphase flow problem. We only mention these different methods briefly here. For a comprehensive review of numerical methods in multiphase flows, the reader is referred to [1–3] and the references given therein.

The Volume-of-Fluid (VOF) method introduced by Hirt and Nicols [4] is designed to be volume conservative even in the discrete case. This is achieved by transporting the sharp

^{*}fricke@mma.tu-darmstadt.de (Corresponding Author)

[†]maric@mma.tu-darmstadt.de

[‡]aleksandar.vuckovic@stud.tu-darmstadt.de

[§]bothe@mma.tu-darmstadt.de

phase indicator function with a finite volume discretization. However, in practice, exact volume conservation may not be achieved (e.g., because of directional splitting and heuristic volume redistribution algorithms to ensure boundedness). The VOF method requires some specialized techniques to numerically transport the sharp discontinuity of the phase indicator function. Geometrical VOF methods (see, e.g., [2, 5]) reconstruct the sharp interface after each transport step in order to prevent numerical diffusion of the interface. In general, the numerical approximation of the interface curvature is known to be challenging for VOF methods, in particular for unstructured meshes [5, 6]. Another important class of methods are front tracking methods (see, e.g., [7]). They represent the interface by a set of connected marker points which are advected by the flow according to an ordinary differential equation. While the accuracy of these methods is potentially very high and the interface stays sharp by construction, there is no built-in phase volume conservation and handling topological changes is expensive.

In the present work, we focus on the level set method due to Osher and Sethian [8–13]. It represents the interface as the zero contour of a smooth function ϕ called the “level set function”

$$\Sigma(t) = \{x \in \Omega : \phi(t, x) = 0\}.$$

Similarly to the VOF method, the level set method is able to handle topological changes naturally. The higher regularity of the level set function compared to the phase indicator function in VOF has some numerical advantages. For example, the interface curvature can be computed more easily. On the other hand, the level set method is not strictly volume conservative in the discrete case. This is a consequence of the fact that the level set ϕ is an auxiliary function that has no physical meaning except for the zero iso-surface representing the interface. Even though, the integral of ϕ over the computational domain is conserved¹ for an incompressible flow, one cannot obtain relevant physical information from this conservation principle in general. If, however, a smoothed Heaviside function is used, this conservation principle becomes the basis for the conservative level set method due to Olsson and Kreiss [14–16] (see below).

A typical example of a level set function is the so-called signed distance function d_Σ associated with a given hypersurface Σ . It is characterized by the property $|\nabla d_\Sigma| = 1$ and has a number of convenient properties (see Appendix A for more details). For example, the mean curvature and normal speed of Σ be computed as the Laplacian and the partial time-derivative, respectively

$$\kappa_\Sigma = \Delta d_\Sigma, \quad V_\Sigma = -\partial_t d_\Sigma.$$

By keeping (at least approximately) the signed distance property, one can assure that the gradients of the level set function become neither too steep nor too flat compared to the computational resolution. This is important for the numerical accuracy and stability of the method. But in fact, the classical level set equation, i.e.

$$\partial_t \phi + v \cdot \nabla \phi = 0, \tag{1}$$

does not preserve the signed distance property, i.e. the norm of the gradient of ϕ will not be constant, not even for the exact solution of (1) and not even at $\phi = 0$. This well-known problem is addressed by “reinitialization” or “redistancing” methods (see [17–19] for some of the first contributions in this direction) that compute a signed distance field from a given fixed zero contour. This recomputed level set is then used to replace the “degenerated” level set function. In many cases, the redistancing is done by solving a PDE in pseudo time. For example, Sussman et al. [17] proposed to solve the initial value problem for the

¹Here we assume that there is no in- or outflow at the domain boundaries. Then $\partial_t \phi + v \cdot \nabla \phi = 0$ implies $\frac{d}{dt} \int_\Omega \phi dV = 0$.

Hamilton-Jacobi equation

$$\frac{\partial}{\partial \tau} \phi + \text{sgn}(\phi^0)(|\nabla \phi| - 1) = 0, \quad \phi|_{\tau=0} = \phi^0 \quad (2)$$

to transform a given level set function ϕ^0 into a signed distance field while keeping the zero contour fixed. In order to save computational time, the redistancing is usually only applied on demand and not at every time step.

There is a particular issue with the redistancing algorithms when the free surface touches the boundary to form a so-called “contact line”. Physically, the contact line (defined as the line of intersection of the free surface with a solid boundary) plays an important role because its presence leads to a variety of additional physical effects that are to be modeled via appropriate boundary conditions. Leaving aside the details of the mathematical modeling, the redistancing algorithm based on (2) faces the problem that additional boundary conditions are required in a region close to the contact line called the “blind spot” [20, 21]. There is no obvious choice for these boundary conditions because it would require a continuation of the zero level set beyond the domain boundary. Della Rocca and Blanquart reported that there are several methods to populate the blind spot which in many cases cause poor calculation of interface curvature and thereby lead to unintended parasitic currents [20, p.35]. Moreover, the redistancing itself may contribute to errors in volume conservation by an unintended motion of the interface [10, 22]. Olsson and Kreiss addressed the problem of phase volume conservation with a level set method [14–16] that aims at transporting a smoothed step function instead of a signed distance function. A compression scheme in pseudo-time is applied in an intermediate step to restore the characteristic width of the transition region after advection. They showed that this strategy is able to improve the phase volume conservation significantly.

There are already some methods available in the literature which try to combine the advection and redistancing of the level set into one single “monolithic” approach [23–31]. Li et al. [23, 24] and later Touré and Soulaïmani [25] introduced a variational formulation where deviations from a signed distance function are penalized in the objective functional. The evolution equation of the level set is then obtained as the corresponding gradient flow to minimize the objective functional. This way the level set function is kept close to a signed distance function during its evolution. However, a displacement of the zero contour with respect to standard level set equation cannot be ruled out completely but is numerically reduced using another penalty term [31]. Coupez et al. introduced the “convected level set method” [26–30] that combines the redistancing equation (2) with the usual advection equation into one single equation. The resulting PDE aims at keeping the level set function close to a signed distance while the motion of the zero contour remains exactly the same on the continuous level (up to discretization errors). Recently, de Luna et al. [31] introduced a conservative monolithic level set method. Similarly to the approach by Li et al., an approximate signed distance function is kept by penalizing deviations from a signed distance. The conservation property is achieved by transporting a smoothed step function similarly to the method by Olsson and Kreiss. Finally, it is also worth mentioning that there have been a lot of developments on hybrid methods that combine ideas and methods from different approaches. The hybrid Level Set / Front Tracking method [32] resolves the challenge of topological interface changes efficiently by tracking the fluid interface as a zero level-set from a signed distance, recovered from the geometrical approximation of the evolving interface in its near vicinity. This way, the interface can be efficiently recovered as a zero-level set in the case of merging or coalescence.

In this work, we introduce a novel transport equation for the level set function that ensures exact conservation of $|\nabla \phi|$ at the zero contour on the continuous level. This is done by introducing a non-linear source term that is derived from the kinematics of interfaces as studied in [33–35]. We show that, in practice, it is sufficient to solve a linear problem in

each timestep. Moreover, the method works naturally with a moving contact line without special treatment. In particular, we demonstrate numerically that the transported contact angle and the curvature at the contact line are nicely converging.

The remainder of this article is organized as follows: The derivation of the level set equation with source term is presented in Section 2. The resulting PDE is then discretized with a simple first-order upwind method in Section 3. First numerical results are discussed in Section 4.

2 A novel level set advection equation

2.1 Problem setup

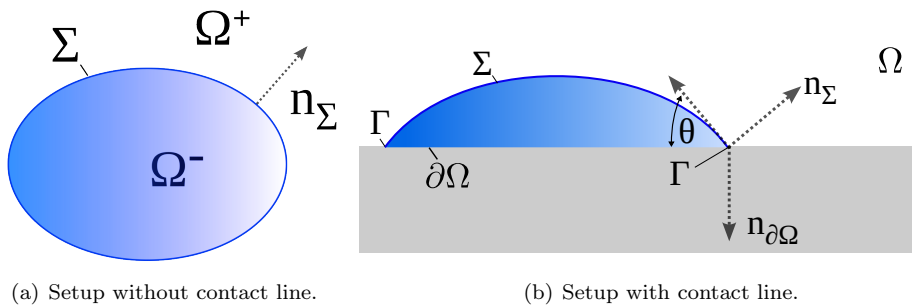


Figure 1: Notation and problem setup.

In the present article, we focus on the problem of *advecting* the fluid interface in a two-phase flow problem. We assume the transporting velocity field as given while keeping in mind that, in applications of the method, it will emerge as a (numerical) solution of the Navier Stokes equations. Mathematically, we consider a domain Ω with piecewise smooth boundary $\partial\Omega$ and velocity field $v = v(t, x)$ that is of class \mathcal{C}^1 on $\mathbb{R} \times \Omega$ and divergence-free (modeling incompressible flow)². Moreover, we consider a \mathcal{C}^2 hypersurface Σ_0 which serves as the initial condition for the advection problem. We assume that Σ_0 is either a closed hypersurface (without boundary) or that its boundary is contained in the domain boundary $\partial\Omega$ (see Fig. 1):

$$\partial\Sigma_0 = \emptyset \quad \text{or} \quad \partial\Sigma_0 \subset \partial\Omega.$$

In the latter case, we call the boundary of the interface the contact line and denote it with the symbol Γ_0 . We do not go into details of the contact line modeling here and only assume that the velocity field v satisfies an impermeability condition at the boundary, i.e.

$$v \cdot n_{\partial\Omega} = 0 \quad \text{at } \partial\Omega, \tag{3}$$

where $n_{\partial\Omega}$ denotes the unit outer normal field to $\partial\Omega$.

Problem statement: Given Σ_0 and $v = v(t, x)$ as described above, find the moving hypersurface

$$\mathcal{M} = \text{gr}(\Sigma) = \bigcup_{t \in \mathbb{R}_+^+} \{t\} \times \Sigma(t) \in \mathcal{C}^1(\mathbb{R} \times \Omega)$$

²Note that in a real two-phase flow problem, the velocity field will only be \mathcal{C}^0 across the interface Σ due to the jump conditions at the interface. Here we assume $v \in \mathcal{C}^1(\mathbb{R} \times \Omega)$ for simplicity.

that satisfies the initial condition

$$\Sigma(0) = \Sigma_0 \quad (4)$$

and the kinematic condition

$$V_\Sigma = v \cdot n_\Sigma \quad \text{on } \text{gr}(\Sigma). \quad (5)$$

Here, the symbol V_Σ denotes the speed of normal displacement of Σ (see Appendix A).

Note that the moving hypersurface \mathcal{M} is uniquely determined by (4) and (5) if the velocity field v is sufficiently regular and tangential to the boundary as required in (3); see [33, 34] for more details. In particular, we emphasize there is no additional boundary condition for the interface orientation to be satisfied. For an introduction to the mathematical modeling of dynamic contact lines, the reader is referred to [36], [37], [34].

So in the standard level set method, we consider the initial value problem

$$\begin{aligned} \partial_t \phi + v \cdot \nabla \phi &= 0, & x \in \Omega, \quad t > 0, \\ \phi(0, x) &= \phi_0(x), & x \in \Omega, \end{aligned}$$

where ϕ_0 is (locally) a signed distance field of Σ_0 and v satisfies (3).

2.2 Preliminary remarks

Definition of the normal field: Note that we can define a natural extension of the normal field away from Σ by means of

$$n = \frac{\nabla \phi}{|\nabla \phi|} \quad (6)$$

as long as $\nabla \phi \neq 0$. Clearly, the extended field will coincide with n_Σ at the zero contour, i.e. $n = n_\Sigma$ at $\phi = 0$.

Rate-of-change of the norm of the gradient: It is well-known that $|\nabla \phi|$ is not conserved. We compute the rate-of-change of $|\nabla \phi|$ explicitly. We use the simply identity

$$2 \left\langle \frac{D}{Dt} \nabla \phi, \nabla \phi \right\rangle = \frac{D}{Dt} |\nabla \phi|^2 = 2 |\nabla \phi| \frac{D}{Dt} |\nabla \phi|. \quad (7)$$

Application of the gradient operator to equation (1) shows that (see [33, 35])

$$\frac{D}{Dt} \nabla \phi = -(\nabla v)^\top \nabla \phi.$$

Hence, it follows that

$$\begin{aligned} \frac{D}{Dt} |\nabla \phi| &= -|\nabla \phi| \left\langle (\nabla v) \frac{\nabla \phi}{|\nabla \phi|}, \frac{\nabla \phi}{|\nabla \phi|} \right\rangle \\ &= -|\nabla \phi| \langle (\nabla v) n_\Sigma, n_\Sigma \rangle =: |\nabla \phi| \mathcal{R}. \end{aligned} \quad (8)$$

Remark 1 (Rate of interface generation). Note that the term

$$\mathcal{R} = \nabla_\Sigma \cdot v = \nabla \cdot v - \langle (\nabla v) n_\Sigma, n_\Sigma \rangle = - \langle (\nabla v) n_\Sigma, n_\Sigma \rangle \quad (9)$$

has an important physical interpretation. In fact, it is nothing but the local rate of *interface generation*. Hence, it measures how much a small control area on the interface is expanded

or compressed while it is transported by the flow. This can be seen from the surface transport theorem for co-moving areas (see Appendix B) as follows

$$\frac{d}{dt}|A(t)| = \frac{d}{dt} \int_{A(t)} d\sigma = \int_{A(t)} \operatorname{div}_{\Sigma} \mathbf{v} d\sigma.$$

Note that, equation (9) implies that the quantity $\langle (\nabla v)n_{\Sigma}, n_{\Sigma} \rangle$ must be continuous across the interface in a two-phase flow setting (since it approaches \mathcal{R} from both sides). Moreover, the function \mathcal{R} has a natural extension away from the interface by means of $n = \nabla \phi / |\nabla \phi|$

$$\mathcal{R} = -\langle (\nabla v)n, n \rangle(t, x) \quad \text{for } \phi \neq 0.$$

2.3 Derivation of the level set advection equation

Motivated by the previous considerations, we derive a transport equation for the level set function that preserves the norm of the gradient at the zero contour. Of course, the dynamics of the zero contour must still be the same as in the standard formulation. To achieve this, we consider the following ansatz

$$\partial_t \phi + v \cdot \nabla \phi = \phi f(\phi, v). \quad (10)$$

Equation (10) leaves the motion of the zero contour invariant provided that f is bounded as $\phi \rightarrow 0$. On the other hand, the function f can be carefully chosen in order to achieve

$$\frac{D}{Dt} |\nabla \phi| \Big|_{\phi=0} = 0. \quad (11)$$

For this purpose, we compute the rate-of-change of $|\nabla \phi|$ for a solution of (10). Application of the gradient operator to a solution of (10) yields

$$\frac{D}{Dt} \nabla \phi = -(\nabla v)^{\top} \nabla \phi + f(\phi, v) \nabla \phi + \phi \nabla f(\phi, v).$$

Hence, we obtain using (7) and $n = \nabla \phi / |\nabla \phi|$

$$\frac{D}{Dt} |\nabla \phi| = |\nabla \phi| (-\langle (\nabla v)n, n \rangle + f) + \phi n \cdot \nabla f. \quad (12)$$

Now, we have to choose f in such a way that the right-hand side of (12) vanishes for $\phi = 0$. Obviously, the choice

$$f(\phi, v) := -\mathcal{R} = \langle (\nabla v)n, n \rangle \quad (13)$$

does the job. In this case, we have

$$\frac{D}{Dt} |\nabla \phi| = -\phi \frac{\partial \mathcal{R}}{\partial n}. \quad (14)$$

In particular, the norm of the gradient of ϕ is preserved at the interface.

Summary: We propose to solve the non-linear equation

$$\partial_t \phi + v \cdot \nabla \phi = \phi \left\langle (\nabla v) \frac{\nabla \phi}{|\nabla \phi|}, \frac{\nabla \phi}{|\nabla \phi|} \right\rangle = -\phi \mathcal{R}. \quad (15)$$

3 An adapted upwind method

In order to construct numerical methods based on (15), we note that a reasonable approximation is to approximate the interface generation rate \mathcal{R} in each time interval $[t^n, t^{n+1}]$ by some function $r = r(t, x)$ that is decoupled from the level set function ϕ . For example, r could be a snapshot of \mathcal{R} at time t^n . Thanks to this approximation, we will consider the *linear* problem

$$\partial_t \phi + v \cdot \nabla \phi = -r(x) \phi, \quad x \in \Omega, \quad t > 0 \quad (16)$$

in each time step. In fact, the zero-contour of the solution of the linear problem (16) coincides with the zero-contour of the non-linear problem (15). Hence, approximating the interface generation rate $\mathcal{R}(t, x)$ by $r(x)$ only leads to deviations in $|\nabla \phi|$ with no impact on the evolution of the zero-contour. Hence, on the continuous level, no accuracy is lost in the position of the interface. On the other hand, small deviations from $|\nabla \phi| = 1$ at the interface are usually unproblematic in practice. Moreover, the normalization of the gradient at the interface is consistently achieved when refining the mesh and the timestep. Therefore, we may concentrate on linear problems of type (16) for the construction of numerical methods.

Remark 2. Using the method of characteristics (see, e.g., [38]), it is easy to show that equation (16) is well-posed as an initial value problem if the velocity field satisfies the impermeability condition

$$v \cdot n_{\partial\Omega} = 0 \quad \text{at } \partial\Omega.$$

The reason is that the characteristics of (1) and (16) are the same. The only difference is that for (16), the function ϕ is no longer constant along characteristics. Hence, no boundary condition has to be imposed for (16) and the kinematics of the contact angle is not affected. This makes this method particularly interesting for the simulation of dynamic wetting problems.

Derivation of the scheme: Integrating (16) over a control volume V_{ijk} yields (assuming $\nabla \cdot v = 0$)

$$\frac{d}{dt} \frac{1}{|V_{ijk}|} \int_{V_{ijk}} \phi dV = \frac{1}{|V_{ijk}|} \int_{\partial V_{ijk}} \phi v \cdot n dA - \frac{1}{|V_{ijk}|} \int_{V_{ijk}} r \phi dV. \quad (17)$$

One of the simplest possible methods to solve (17) is the first-order upwind scheme. It can be seen as a primer for more sophisticated methods with a higher order of accuracy. In order to derive it, we may approximate the last term as

$$\frac{1}{|V_{ijk}|} \int_{V_{ijk}} r \phi dV \approx \left(\frac{1}{|V_{ijk}|} \int_{V_{ijk}} r dV \right) \left(\frac{1}{|V_{ijk}|} \int_{V_{ijk}} \phi dV \right).$$

With this approximation, we obtain a particularly well-suited problem to be solved with finite volume methods

$$\frac{d}{dt} \frac{1}{|V_{ijk}|} \int_{V_{ijk}} \phi dV = \frac{1}{|V_{ijk}|} \int_{\partial V_{ijk}} \phi v \cdot n dA - \left(\frac{1}{|V_{ijk}|} \int_{V_{ijk}} r dV \right) \left(\frac{1}{|V_{ijk}|} \int_{V_{ijk}} \phi dV \right). \quad (18)$$

A simple time-explicit semi-discretization of (18) reads as

$$\begin{aligned} \frac{\phi_{ijk}^{n+1} - \phi_{ijk}^n}{\Delta t} &= \mathcal{F}_{ijk}^n - r_{ijk}^n \phi_{ijk}^n \\ \Leftrightarrow \phi_{ijk}^{n+1} &= \phi_{ijk}^n (1 - r_{ijk}^n \Delta t) + \Delta t \mathcal{F}_{ijk}^n. \end{aligned} \quad (19)$$

where \mathcal{F}_{ijk}^n denotes the total (sum over all faces) upwind flux³ for the control volume V_{ijk} at time t_n and r_{ijk}^n is a discretization of the rate of interface generation. Hence, the only implementation work needed to extend the standard upwind scheme for (15) is to discretize the source term

$$r_{ijk}^n = -\langle (\nabla v) n, n \rangle_{ijk}^n = -\left\langle (\nabla v) \frac{\nabla \phi}{|\nabla \phi|}, \frac{\nabla \phi}{|\nabla \phi|} \right\rangle_{ijk}^n$$

and to include it the time integration according to (19). For the purpose of this demonstrator method, we take the analytical velocity gradient at the cell center and discretize $\nabla \phi$ with second-order central finite differences away from the boundary. At boundaries, we use the second-order forward-/backward finite difference schemes

$$\begin{aligned} f'(x) &= \frac{-3f(x) + 4f(x + \Delta x) - f(x + 2\Delta x)}{2\Delta x} + \mathcal{O}(\Delta x^2), \\ f'(x) &= \frac{3f(x) - 4f(x - \Delta x) + f(x - 2\Delta x)}{2\Delta x} + \mathcal{O}(\Delta x^2). \end{aligned} \tag{20}$$

Second-order accuracy is reached if the function f is of class \mathcal{C}^3 .

Remark 3 (Regularization of the source term). Obviously, the source term r_{ijk}^n is not well-defined if $|\nabla \phi| = 0$. Therefore, it must be regularized in these regions. To achieve this, we replace

$$\frac{\nabla \phi}{|\nabla \phi|} \quad \text{by} \quad \frac{\nabla \phi}{|\nabla \phi| + \varepsilon}$$

for some small regularization parameter ε . This will affect the calculation of the normal vector only in regions where $|\nabla \phi|$ is already very small. We use $\varepsilon = 10^{-12}$ for our numerical experiments in Section 4.

The method described above is implemented in a C++ demonstrator code that has been published before (without the source term) as Open Source in [40, 41].

4 Numerical examples

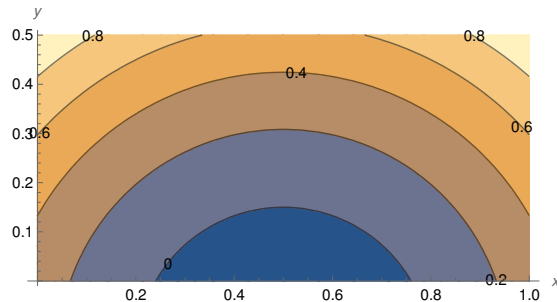


Figure 2: Iso-contours of the initial level set ϕ_0 .

We consider a two-dimensional domain

$$0 \leq x \leq 1, \quad 0 \leq y \leq 0.5$$

and consider the initial level set function (see Fig. 2)

$$\phi_0(x, y) = \frac{1}{2} \left(\frac{(x - x_0)^2}{R_0} + \frac{(y - y_0)^2}{R_0} - R_0 \right)$$

³See [39] for a discussion of the first-order upwind method.

for $x_0 = 0.5$, $y_0 = -0.15$ and $R_0 = 0.3$. Hence, the initial zero contour is a semi-circle that meets the boundary $y = 0$ at a contact angle of 60 degrees. Note that ϕ_0 is designed in such a way that $|\nabla\phi_0| = 1$ holds at the zero contour. For the spatial discretization, we use a uniform cartesian grid with $\Delta x = \Delta y$. We chose between 50 and 200 cells in the x -direction corresponding to between 15 and 60 cells per initial radius R_0 .

Two velocity fields are chosen to transport the level set with the first-order upwind scheme

- (i) “Vortex-in-a-box field”:

$$v(x, y) = v_0(-\sin(\pi x) \cos(\pi y), \cos(\pi x) \sin(\pi y)) \quad (21)$$

for $v_0 = -0.2$.

- (ii) “Time-periodic field”:

$$v(t, x, y) = \cos\left(\frac{\pi t}{\tau}\right) (v_0 + c_1 x + c_2 y, -c_1 y) \quad (22)$$

for $v_0 = -0.2$, $c_1 = 0.1$, $c_2 = -2$ and $\tau = 0.4$.

The mesh size is varied to study the numerical convergence of the method. The numerical timestep is varied accordingly such that the CFL number is kept constant (CFL = 0.5 in this case).

We study the evolution of the “right” contact point, initially being located at coordinate $x = x_0 + R \sin \theta_0 = 0.5 + 0.3 \sin(60^\circ) \approx 0.76$. We follow this point along the $y = 0$ boundary and evaluate

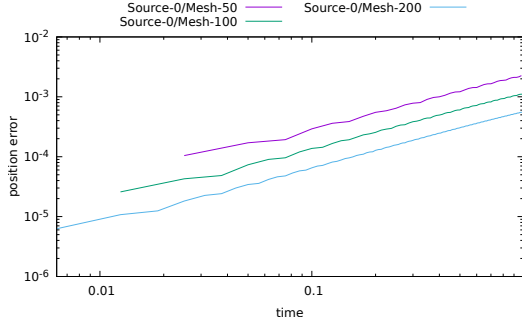
- (i) the coordinate $x(t)$,
- (ii) the contact angle $\theta(t)$,
- (iii) the curvature $\kappa(t)$ and
- (iv) the norm of the gradient $|\nabla\phi|(t)$ for the standard level set method and the new version with active source term.

For the transport of the coordinate $x(t)$ as well as the contact angle $\theta(t)$, we have access to reference solutions derived in [33, 42]. In particular, we use the kinematic evolution equation for the dynamic contact angle [33] and the kinematic evolution equation for the curvature in 2D (see [34]) to study the accuracy of the method.

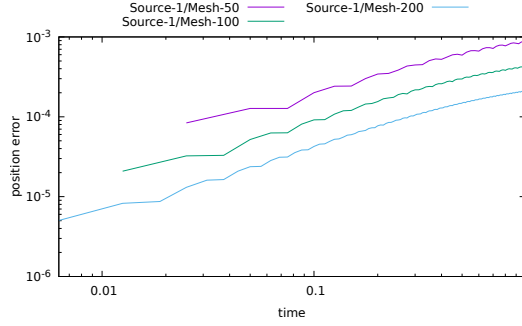
First results: As expected from the results in a previous publication [40], the numerical error for the transport of both the contact point position and the contact angle converges with first-order in time for the standard upwind method; see Figure 3. This is true regardless if the source term is active or not. On the finest mesh, the maximum error for the contact angle is about 0.1 degrees over the considered simulation time. Notably, also the transported curvature converges with mesh refinement.

Figure 4 compares the numerical transport of the position, the contact angle, and the curvature at the contact point on a fine mesh for the standard method and the adapted upwind method with active source term. We observe that the results are practically indistinguishable for the position and the contact angle. A minor deviation is found for the curvature. This indicates that indeed no accuracy is lost in terms of the transport of the zero level set and the normal field. A major difference is, however, observed when we look at the numerical evolution of $|\nabla\phi|$ at the contact point reported in Fig. 4(d). While $|\nabla\phi(t)|$ converges to a monotonically growing function (which is determined by equation (8)) for the standard upwind scheme, we find a converge towards $|\nabla\phi(t)| = 1$ for the new method with active source term.

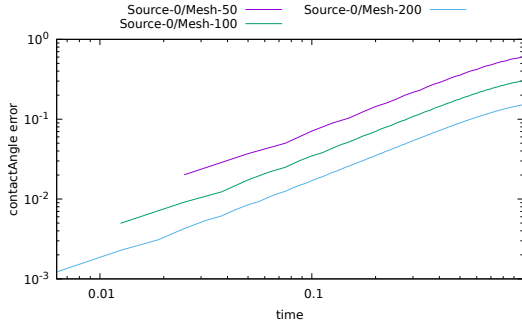
Moreover, by looking at Figure 5, we see that the same is found for the time-periodic example (22). In summary, the simple adapted upwind method (19) seems to work as expected. However, we note that these are preliminary results and a more extensive study will be performed in the future.



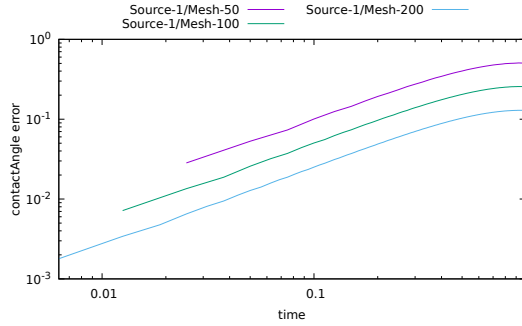
(a) Error $x(t)$ (source off).



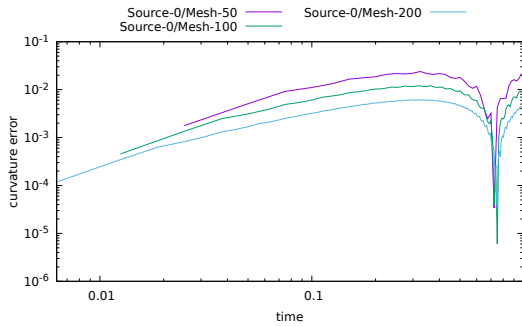
(b) Error $x(t)$ (source on).



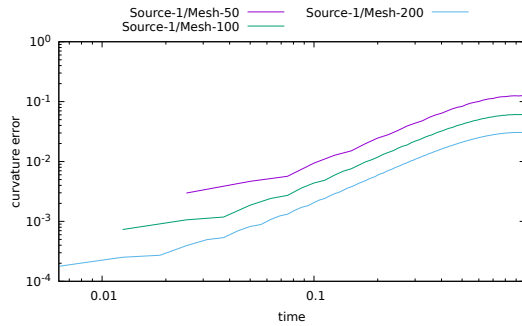
(c) Error $\theta(t)$ (source off).



(d) Error $\theta(t)$ (source on).

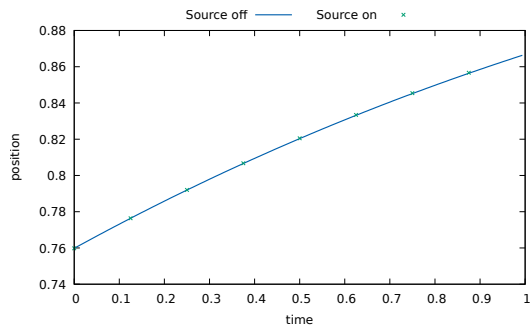


(e) Error $\kappa(t)$ (source off).

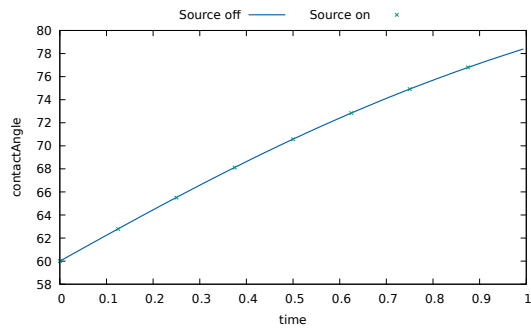


(f) Error $\kappa(t)$ (source on).

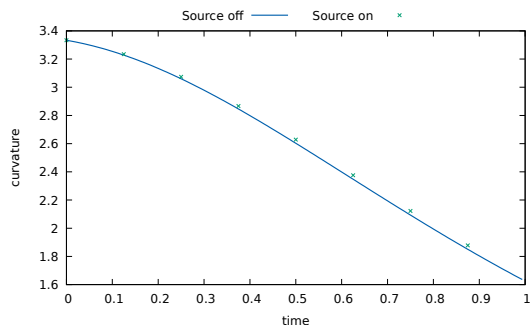
Figure 3: Convergence study for the contact point position and the contact angle. Standard upwind method and vortex-in-a-box field (21).



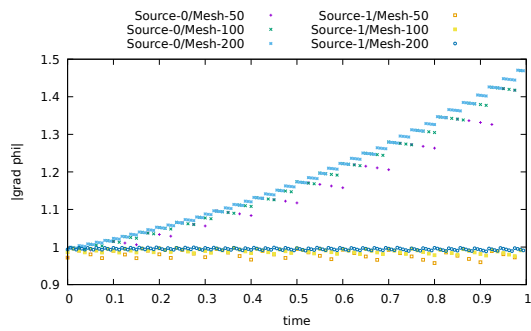
(a) Contact point $x(t)$.



(b) Contact angle $\theta(t)$.

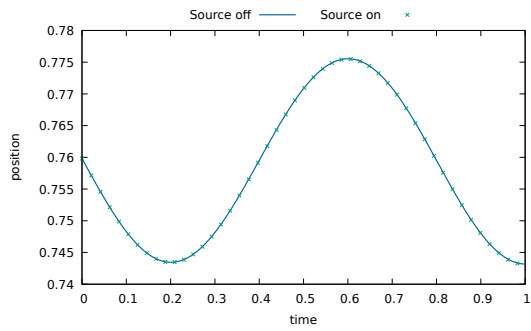


(c) Curvature $\kappa(t)$.

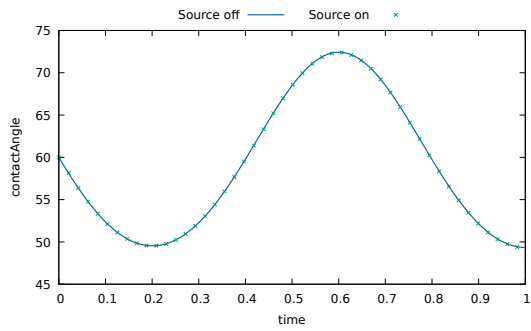


(d) Gradient norm $|\nabla\phi|(t)$.

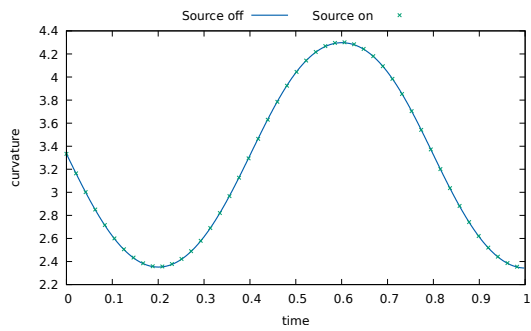
Figure 4: Numerical transport of the contact point position, contact angle, curvature, and gradient norm for the vortex-in-a-box field (21).



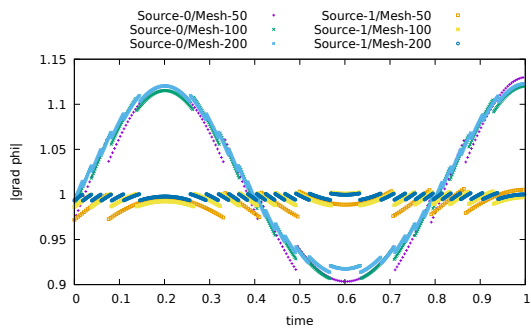
(a) Contact point $x(t)$.



(b) Contact angle $\theta(t)$.



(c) Curvature $\theta(t)$.



(d) Gradient norm $|\nabla\phi|(t)$.

Figure 5: Numerical transport of the contact point position, contact angle, curvature, and gradient norm for time-periodic field (22).

5 Conclusion and outlook

To summarize, we have introduced a novel level set transport equation that intrinsically preserves the norm of the gradient, i.e. $|\nabla\phi|$, at the physical interface represented by the zero contour of ϕ . This is achieved by introducing a source term on the right-hand side which, however, turns the linear hyperbolic problem into a non-linear one. It is important to note that the source term is proportional to the physical rate of interface generation.

In practice, one can avoid solving the non-linear equation (15) by approximating the interface generation by its snapshot at the previous time-step. This way, the problem is approximated by a linear hyperbolic problem of the form

$$\partial_t\phi + v \cdot \nabla\phi = -r(x)\phi. \quad (23)$$

Equation (23) has a number of convenient properties. In particular, the zero contours of (23) and the original level set equation ($r = 0$) are exactly the same. Hence, no source of error for the interface motion is introduced on the continuous level. Moreover, the problem (23) is well-posed in the presence of a moving contact line without the need to impose a boundary condition for ϕ . Hence, the signed distance preserving level set method works without special treatment in the case of a moving contact line. This is particularly interesting because some conventional redistancing methods are showing difficulties in the presence of a contact line. Finally, equation (23) can readily be solved with standard numerical methods. We demonstrated this with the first-order upwind method which requires very little implementation work. First numerical examples show that the accuracy of the original upwind method is retained in terms of the interface position, the contact angle as well as the curvature, while the norm of the gradient at the interface converges to a constant value over time as the mesh is refined.

Altogether, a first proof of concept for the locally signed distance preserving level set method (SDPLS) is established. Starting from here, we will work on an implementation in higher-order level set method and consider the coupling to a two-phase Navier Stokes solver. Among other things, it will be interesting to study if the method has any impact on the numerical conservation of the phase volume.

Acknowledgements: Funded by the Deutsche Forschungsgemeinschaft (DFG, German Research Foundation) – Project-ID 265191195 – SFB 1194.

The authors gratefully acknowledge the computing time provided to them on the high-performance computer Lichtenberg at the NHR Centers NHR4CES at TU Darmstadt. This is funded by the Federal Ministry of Education and Research, and the state governments participating on the basis of the resolutions of the GWK for national high performance computing at universities (www.nhr-verein.de/unsere-partner).

References

- [1] R. Scardovelli and S. Zaleski. Direct Numerical Simulation of Free-Surface and Interfacial Flow. *Annual Review of Fluid Mechanics*, 31(1):567–603, 1999. doi:10.1146/annurev.fluid.31.1.567.
- [2] G. Tryggvason, R. Scardovelli, and S. Zaleski. *Direct numerical simulations of gas-liquid multiphase flows*. Cambridge University Press, 2011. doi:10.1017/CB09780511975264.
- [3] S. Gross and A. Reusken. *Numerical Methods for Two-phase Incompressible Flows*, volume 40 of *Springer Series in Computational Mathematics*. Springer Berlin Heidelberg, Berlin, Heidelberg, 2011. doi:10.1007/978-3-642-19686-7.
- [4] C. W. Hirt and B. D. Nichols. Volume of fluid (VOF) method for the dynamics of free boundaries. *Journal of Computational Physics*, 39(1):201–225, 1981. doi:10.1016/0021-9991(81)90145-5.
- [5] T. Marić, D. B. Kothe, and D. Bothe. Unstructured un-split geometrical Volume-of-Fluid methods – A review. *Journal of Computational Physics*, 420:109695, nov 2020. doi:10.1016/j.jcp.2020.109695.
- [6] S. Popinet. Numerical Models of Surface Tension. *Annual Review of Fluid Mechanics*, 50(1):49–75, 2018. doi:10.1146/annurev-fluid-122316-045034.
- [7] S. O. Unverdi and G. Tryggvason. A front-tracking method for viscous, incompressible, multi-fluid flows. *Journal of Computational Physics*, 100(1):25–37, may 1992. doi:10.1016/0021-9991(92)90307-k.
- [8] S. Osher and J. A. Sethian. Fronts propagating with curvature-dependent speed: Algorithms based on hamilton-jacobi formulations. *Journal of Computational Physics*, 79(1):12–49, nov 1988. doi:10.1016/0021-9991(88)90002-2.
- [9] J.A. Sethian. Evolution, implementation, and application of level set and fast marching methods for advancing fronts. *Journal of Computational Physics*, 169(2):503–555, may 2001. doi:10.1006/jcph.2000.6657.
- [10] S. Osher and R. Fedkiw. *Level Set Methods and Dynamic Implicit Surfaces*. Springer New York, 2003. doi:10.1007/b98879.
- [11] J. A. Sethian and P. Smereka. Level set methods for fluid interfaces. *Annual Review of Fluid Mechanics*, 35(1):341–372, jan 2003. doi:10.1146/annurev.fluid.35.101101.161105.
- [12] F. Gibou, R. Fedkiw, and S. Osher. A review of level-set methods and some recent applications. *Journal of Computational Physics*, 353:82–109, jan 2018. doi:10.1016/j.jcp.2017.10.006.
- [13] Y. Giga. *Surface evolution equations: A level set approach*, volume 99 of *Monographs in Mathematics*. Birkhäuser, Basel, 2006. doi:10.1007/3-7643-7391-1.
- [14] E. Olsson and G. Kreiss. A conservative level set method for two phase flow. *Journal of Computational Physics*, 210(1):225–246, nov 2005. doi:10.1016/j.jcp.2005.04.007.
- [15] E. Olsson, G. Kreiss, and S. Zahedi. A conservative level set method for two phase flow II. *Journal of Computational Physics*, 225(1):785–807, jul 2007. doi:10.1016/j.jcp.2006.12.027.
- [16] S. Zahedi, K. Gustavsson, and G. Kreiss. A conservative level set method for contact line dynamics. *Journal of Computational Physics*, 228(17):6361–6375, sep 2009. doi:10.1016/j.jcp.2009.05.043.
- [17] M. Sussman, P. Smereka, and S. Osher. A level set approach for computing solutions to incompressible two-phase flow. *Journal of Computational Physics*, 114(1):146–159, sep 1994. doi:10.1006/jcph.1994.1155.

- [18] J. A. Sethian. A fast marching level set method for monotonically advancing fronts. *Proceedings of the National Academy of Sciences*, 93(4):1591–1595, 1996. doi:10.1073/pnas.93.4.1591.
- [19] M. Sussman and E. Fatemi. An efficient, interface-preserving level set redistancing algorithm and its application to interfacial incompressible fluid flow. *SIAM Journal on Scientific Computing*, 20(4):1165–1191, jan 1999. doi:10.1137/s1064827596298245.
- [20] G. Della Rocca and G. Blanquart. Level set reinitialization at a contact line. *Journal of Computational Physics*, 265:34–49, may 2014. doi:10.1016/j.jcp.2014.01.040.
- [21] S. Pertant, M. Bernard, G. Ghigliotti, and G. Balarac. A finite-volume method for simulating contact lines on unstructured meshes in a conservative level-set framework. *Journal of Computational Physics*, 444:110582, nov 2021. doi:10.1016/j.jcp.2021.110582.
- [22] Z. Solomenko, P. D.M. Spelt, and P. Alix. A level-set method for large-scale simulations of three-dimensional flows with moving contact lines. *Journal of Computational Physics*, 348:151–170, nov 2017. doi:10.1016/j.jcp.2017.07.011.
- [23] C. Li, C. Xu, C. Gui, and M.D. Fox. Level set evolution without re-initialization: A new variational formulation. In *2005 IEEE Computer Society Conference on Computer Vision and Pattern Recognition (CVPR'05)*. IEEE, 2005. doi:10.1109/cvpr.2005.213.
- [24] C. Li, C. Xu, K. M. Konwar, and M. D. Fox. Fast distance preserving level set evolution for medical image segmentation. In *2006 9th International Conference on Control, Automation, Robotics and Vision*. IEEE, 2006. doi:10.1109/icarcv.2006.345357.
- [25] M. Kabirou Touré and A. Soulaïmani. Stabilized finite element methods for solving the level set equation without reinitialization. *Computers and Mathematics with Applications*, 71(8):1602–1623, apr 2016. doi:10.1016/j.camwa.2016.02.028.
- [26] L. Ville, L. Silva, and T. Coupez. Convected level set method for the numerical simulation of fluid buckling. *International Journal for Numerical Methods in Fluids*, 66(3):324–344, apr 2011. doi:10.1002/flid.2259.
- [27] T. Coupez. Convection of local level set function for moving surfaces and interfaces in forming flow. In *AIP Conference Proceedings*. AIP, 2007. doi:10.1063/1.2740790.
- [28] C. Bahbah, M. Khalloufi, A. Larcher, Y. Mesri, T. Coupez, R. Valette, and E. Hachem. Conservative and adaptive level-set method for the simulation of two-fluid flows. *Computers & Fluids*, 191:104223, sep 2019. doi:10.1016/j.compfluid.2019.06.022.
- [29] Malú Grave, José J. Camata, and Alvaro L.G.A. Coutinho. A new convected level-set method for gas bubble dynamics. *Computers & Fluids*, 209:104667, sep 2020. doi:10.1016/j.compfluid.2020.104667.
- [30] A. Bonito, J.-L. Guermond, and S. Lee. Numerical simulations of bouncing jets. *International Journal for Numerical Methods in Fluids*, 80(1):53–75, jul 2015. doi:10.1002/flid.4071.
- [31] M. Q. de Luna, D. Kuzmin, and C. E. Kees. A monolithic conservative level set method with built-in redistancing. *Journal of Computational Physics*, 379:262–278, feb 2019. doi:10.1016/j.jcp.2018.11.044.
- [32] S. Shin, I. Yoon, and D. Juric. The local front reconstruction method for direct simulation of two- and three-dimensional multiphase flows. *Journal of Computational Physics*, 230(17):6605–6646, jul 2011. doi:10.1016/j.jcp.2011.04.040.
- [33] M. Fricke, M. Köhne, and D. Bothe. A kinematic evolution equation for the dynamic contact angle and some consequences. *Physica D: Nonlinear Phenomena*, 394:26–43, 2019. doi:10.1016/j.physd.2019.01.008.

- [34] M. Fricke. *Mathematical Modeling and Volume-of-Fluid based simulation of dynamic wetting*. PhD thesis, TU Darmstadt, 2021. doi:10.12921/tuprints-00014274.
- [35] M. Fricke, M. Köhne, and D. Bothe. On the kinematics of contact line motion. *PAMM*, 18(1):e201800451, 2018. doi:10.1002/pamm.201800451.
- [36] D. Bonn, J. Eggers, J. Indekeu, J. Meunier, and E. Rolley. Wetting and spreading. *Reviews of Modern Physics*, 81(2):739–805, 2009. doi:10.1103/RevModPhys.81.739.
- [37] Y. D. Shikhmurzaev. *Capillary flows with forming interfaces*. Chapman & Hall/CRC, Boca Raton, 2008. doi:10.1201/9781584887492.
- [38] L. C. Evans. *Partial Differential Equations*. American Mathematical Society, Providence, R.I., 2010.
- [39] R. J. LeVeque. *Finite Volume Methods for Hyperbolic Problems*. Cambridge University Press, Cambridge, 2002. doi:10.1017/CB09780511791253.
- [40] M. Fricke, T. Marić, and D. Bothe. Contact Line Advection using the Level Set Method. *PAMM*, 19(1):e201900476, 2019. doi:10.1002/pamm.201900476.
- [41] M. Fricke, T. Marić, A. Vučković, and D. Bothe. Contact Line Advection using the Level Set Method: Data and C++-Implementations, 2019. doi:10.25534/tudatalib-58.
- [42] M. Fricke, T. Marić, and D. Bothe. Contact Line Advection using the geometrical Volume of Fluid Method. *Journal of Computational Physics*, 2020. doi:10.1016/j.jcp.2019.109221.
- [43] M. Kimura. Geometry of hypersurfaces and moving hypersurfaces in \mathbb{R}^m - for the study of moving boundary problems. In M. Benes and E. Feireisl, editors, *Jindřich Nečas Center for Mathematical Modeling, Lecture notes Volume IV, Topics in Mathematical Modeling*, pages 39–93. matfyzpress, Prague, 2008.
- [44] J. Prüss and G. Simonett. *Moving interfaces and quasilinear parabolic evolution equations*. Monographs in Mathematics. Birkhäuser, Switzerland, 2016. doi:10.1007/978-3-319-27698-4.
- [45] R. Aris. *Vectors, tensors and the basic equations of fluid mechanics*. Dover Publications, New York, 1989.
- [46] D. Bothe, J. Prüss, and G. Simonett. Well-posedness of a two-phase flow with soluble surfactant. In Haim Brezis, Michel Chipot, and Joachim Escher, editors, *Nonlinear Elliptic and Parabolic Problems*, Progress in Nonlinear Differential Equations and Their Applications, pages 37–61. Birkhäuser, Basel, 2005. doi:10.1007/3-7643-7385-7_3.

A Preliminaries on (moving) interfaces

We briefly recall some basic mathematical definitions for (moving) hypersurfaces; see [13, 43, 44] for more details.

Construction of the signed distance function (see Chapter 2.3 in [44]): Mathematically, the signed distance function d_Σ is constructed by inverting the map

$$h \mapsto x + hn_\Sigma(x)$$

for some point x on the interface Σ .

Lemma 1. *Let $\Sigma \subset \mathbb{R}^d$ be a \mathcal{C}^2 -hypersurface and x_0 be an inner point of Σ . Then there exists an open neighborhood $U \subset \mathbb{R}^n$ of x_0 and $\varepsilon > 0$ such that the map*

$$\begin{aligned} X : (\Sigma \cap U) \times (-\varepsilon, \varepsilon) &\rightarrow \mathbb{R}^n \\ X(x, h) &:= x + hn_\Sigma(x) \end{aligned}$$

is a diffeomorphism onto its image

$$\mathcal{N}^\varepsilon := X((\Sigma \cap U) \times (-\varepsilon \times \varepsilon)) \subset \mathbb{R}^n,$$

i.e. X is invertible there and both X and X^{-1} are \mathcal{C}^1 . The inverse function has the form

$$X^{-1}(x) = (\pi_\Sigma(x), d_\Sigma(x)) \quad (24)$$

with \mathcal{C}^1 -functions π_Σ and d_Σ on \mathcal{N}^ε .

In fact, the signed distance function is defined only locally on the so-called ‘‘tubular neighborhood’’ \mathcal{N}^ε . The operator π_Σ in (24) is the projection operator that maps each point $x \in \mathcal{N}^\varepsilon$ to its ‘‘base point’’ $\pi_\Sigma(x)$ located at the signed distance $d_\Sigma(x)$. Moreover, one can show that [44]

$$\nabla d_\Sigma|_\Sigma = n_\Sigma \quad (25)$$

which implies that

$$|\nabla d_\Sigma| = |n_\Sigma| = 1 \quad \text{on } \Sigma. \quad (26)$$

As a consequence, the mean curvature of the interface can simply be computed as

$$\kappa = -\Delta d_\Sigma \quad \text{at } \Sigma. \quad (27)$$

Moving hypersurfaces: Similar definitions of a moving hypersurface can also be found in [13, 43, 44]. A generalization to moving hypersurfaces with boundary is given in [33].

(a) Let $I = (a, b)$ be an open interval. A family $\{\Sigma(t)\}_{t \in I}$ with $\Sigma(t) \subset \mathbb{R}^3$ is called a $\mathcal{C}^{k,m}$ -family of moving hypersurfaces if the following holds.

- (i) Each $\Sigma(t)$ is an orientable \mathcal{C}^m -hypersurface in \mathbb{R}^3 with unit normal field denoted as $n_\Sigma(t, \cdot)$.
- (ii) The graph of Σ , given as

$$\mathcal{M} := \text{gr } \Sigma = \bigcup_{t \in I} \{t\} \times \Sigma(t) \subset \mathbb{R} \times \mathbb{R}^3, \quad (28)$$

is a \mathcal{C}^k -hypersurface in $\mathbb{R} \times \mathbb{R}^3$.

(iii) The unit normal field is k -times continuously differentiable on \mathcal{M} , i.e.

$$n_\Sigma \in \mathcal{C}^k(\mathcal{M}).$$

(b) Let $x_0 \in \Sigma(t_0)$ and $\gamma : I \rightarrow \mathbb{R}^3$ be a \mathcal{C}^1 -curve on $\text{gr } \Sigma$ that passes through x_0 , i.e.

$$\gamma(t_0) = x_0 \quad \text{and} \quad (t, \gamma(t)) \in \text{gr } \Sigma \quad \forall t \in I.$$

Then, the *normal speed* of $\Sigma(t_0)$ at x_0 is defined as

$$V_\Sigma(t_0, x_0) := \gamma'(t_0) \cdot n_\Sigma(t_0, x_0) \in \mathbb{R}. \quad (29)$$

Note that the normal speed defined above does not depend on the choice of γ (see [44] for details).

B Surface transport theorem

We briefly recall the surface transport theorem for two-phase flow (see, e.g. [45, 46]). Let $\{\Sigma(t)\}_{t \in I}$ be a family of moving surfaces and $\mathbf{v}^\Sigma : \text{gr}(\Sigma) \rightarrow \mathbb{R}^3$ a consistent surface velocity field, i.e. \mathbf{v}^Σ satisfies

$$v^\Sigma \cdot n_\Sigma = V_\Sigma \quad \text{on } \text{gr } \Sigma.$$

Let $\{A(t)\}_{t \in I}$ be a co-moving control area inside $\Sigma(\cdot)$ and $\Phi^\Sigma : \text{gr}(\Sigma) \rightarrow \mathbb{R}$ such that $\frac{D^\Sigma \phi^\Sigma}{Dt}$ exists. Then

$$\frac{d}{dt} \int_{A(t)} \phi^\Sigma(t, \mathbf{x}) d\mathbf{o} = \int_{A(t)} \left(\frac{D^\Sigma \phi^\Sigma}{Dt}(t, \mathbf{x}) + \phi^\Sigma \text{div}_\Sigma \mathbf{v}^\Sigma(t, \mathbf{x}) \right) d\mathbf{o}$$

This yields the following relation for co-moving areas

$$\frac{d}{dt} |A(t)| = \frac{d}{dt} \int_{A(t)} d\mathbf{o} = \int_{A(t)} \text{div}_\Sigma \mathbf{v}^\Sigma d\mathbf{o}.$$